

Karolina SADKO

Kielce University of Technology, Poland

Corresponding author: ksadko@tu.kielce.pl

Doi: 10.53412/jntes-2023-2-3

EXPERIMENTAL ANALYSIS OF HEAT FLUX DISTRIBUTION IN TRIPLE-PANE WINDOWS WITHIN A CLIMATIC CHAMBER

Abstract: *An experimental study was carried out to investigate the heat flux distribution on the external surface of triple-pane windows under various conditions including: outdoor temperatures, gas filling, emissivity of the glass surfaces, and the use of electrical heating. The measurements were conducted within a controlled climatic chamber. Two window configurations were examined: one filled with air (emissivity of $\varepsilon = 0.84$) and the other filled with argon (emissivity of $\varepsilon = 0.17$). In addition, the study also assessed the impact of a local and surface electric heating on heat loss. The key contribution of this research lies in revealing variations in the heat flux density across different parts of the external glazing of each window, specifically the lower, central, and upper regions. These findings emphasize the importance of considering the non-uniformity of thermal resistance in different areas of windows in order to accurately determine their heat transfer coefficient.*

Keywords: *heat transfer, heat flux, windows, triple-pane windows, thermal transmittance*

Introduction

Windows and glazed facades are crucial components of building that impact the energy efficiency, visual and acoustic comfort of residents as well as thermal performance. However, up to 60% of total heat loss through the building envelope can be attributed to the glazed areas due to their comparably higher overall heat transfer coefficient (U -value) [1]. Therefore, enhancing the thermal resistance (R -value) of glazed building partitions holds great potential for substantial increase of energy savings.

One of the possible ways of decreasing the thermal transmittance of windows is the utilization of triple-pane windows. The thermal resistance of a triple-pane window filled with air is approximately 1.7 times higher than that of a double-pane window of the same size [2]. The central pane in the triple-pane window causes reduction in velocity of free-convective flow of gas in the gap between panes resulting in higher thermal resistance. As gas rises along the room-side pane surface facing the gap, it changes the flow direction in the upper part of the window and descends along the cold pane surface facing the gap, thus creating a primary circulation. Moreover, micro-convection in the form of secondary multicellular circulations occurs in the gaps of multi-pane windows at the critical Rayleigh number values, therefore causing the degradation of linear temperature profiles. It was found that the Rayleigh number, at which a multicellular flow occurs, is ranging from 6.070 to 6.740 [3]. A similar conclusion was established in paper [4]. The suppression of multicellular flow in the layers of gas between panes occurred when the number of panes increased from two to three. The lower temperature gradient between cavity surfaces was observed in triple-pane windows, resulting in the reduction of buoyancy force in the gas layers. Additionally, the central pane behaves as a screen, decreasing the radiative heat exchange. Another solution to reduce the heat transfer by radiation is an application of low emissivity coatings to the pane surfaces [5]. Replacing air with low thermal conductivity gases such as argon to fill the window gaps can lead to the reduction of conductive and convective heat fluxes [6]. The distribution of the density of heat

fluxes on the glazing surfaces is therefore influenced by the phenomena of convection, conduction and radiation, as well as the materials used in the windows. The level of heat flow passing through the area closest to the window edges differs significantly from the one most proximal to the central area. Both the materials used for making window frames as well as those utilized in the production of insulating layers between the panes in the areas near the glass edges have a higher thermal conductivity than the gas layers in the gaps between the panes. As a consequence, the U -value is not exclusively dependent on the window's surface area, but on the ratio between the central glazed area and the peripheral section [7]. The energy saving that could be achieved by replacing double-pane windows with triple, and quadruple-pane windows was studied in paper [8]. It has been proven that the temperature difference and the number of panes had a greater impact on the heat flux densities than the width of the gap between the panes. A glazing distance of 18 mm in combination with an external temperature of 5°C resulted in an almost 150 W/m² heat loss measure for a double-pane window, dropping to 70 W/m² for a triple-pane window. The decrease was even more not able when an external temperature amounted to 15°C. In that instance, the heat loss was reduced from 200 W/m² to 90 W/m² for a triple-pane window. However, the heat fluxes were obtained for the average and constant values of the inner and outer pane surface temperatures. It was possible due to the fact that convective heat transfer resistance in the inner and outer panes was not considered. Aguilar-Santana et al. utilized the heat flux meter method (ISO 9869-1:2014) to investigate temperatures and heat flow on the glazing surface of active insulated windows [9]. Experimental tests were carried out using the heat flux meters attached to the center of the pane. Furthermore, three temperature stations were placed at the window edges in order to assess the thermal transmittance in the weakest points of tested windows. The results showed that, for an interior chamber temperature of approximately 3.0°C and an external ambient temperature of 12.0°C, the heat flux through the central part of argon-filled double-pane window ranged from 22 W/m² to 28 W/m², resulting in a U -value of 3.09 W/m²·K. Moreover, the measurements confirmed higher thermal transmittance near the lower and upper areas of each window. The highest U -value of 1.48 W/m²·K was registered at the top corner station of the tested vacuum window, whilst the bottom corner station recorded 1.33 W/m²·K. Thus, compared to the central part of the window, where the measured U -value was 1.12 W/m²·K, the values obtained in the upper and lower parts were 32% and 19% higher, respectively. Similarly, Cuce's research [10] on argon-filled double-pane windows in environmental chamber tests revealed varying U -values of 1.25, 1.18 and 1.32 W/m²·K for the top, center, and lower parts of the window, respectively, emphasizing the influence of boundary effects and thermal bridges on heat flux density distribution. The lowest values of the heat flux density in the central part of the window were also confirmed by experimental studies carried out by Pavlenko and Sadko [11]. The study analyzed heat flow patterns in windows with electric heating in an occupied house, considering the operating temperature, location, and orientation [12]. It also compared temperature and dew point distribution profiles with input power values set accordingly to the varying operating temperature conditions of the heated glazing. The influence of solar irradiation resulted in diverse heat flow patterns, and temperature sensor measurements exhibited significant differences from the average temperature at the center of the heated window. The heat flux distribution for each pane of triple-glazed supply-air window was experimentally estimated in [13]. It was pointed out that due to the high thermal conductivity of glass, relying solely on thermocouples is inadequate. However, using heat flux meters at different window heights made it possible to determine the variation of heat flux in different parts of the glazing surface. In situ measurements are widely employed to evaluate the actual thermophysical properties of building elements, offering higher accuracy than other approaches, mainly based on tabulated data. However, this method's extensive financial and time requirement limit its widespread use [14].

The heat transfer through windows is characterized by very complex physical phenomena leading to variations heat flux density across different parts of the window. This experimental research aims to determine the heatflux densities on the lower, central, and upper parts of external surfaces of triple-pane windows within a climatic chamber. The study compares heat flux density distributions, U -values, and R -values of both air- and argon-filled windows, considering the use of low-emissivity coatings and electric heating.

Materials and Methods

Materials

The experimental study was conducted at the Laboratory of Material Structure and Heat Exchange at the Kielce University of Technology (Poland), using a climatic chamber. The climatic chamber consists of two boxes: an internal (hot) box measuring $2.25\text{ m} \times 1.8\text{ m} \times 2.30\text{ m}$, simulating indoor conditions with adjustable temperatures ranging from $+5\text{ }^{\circ}\text{C}$ to $+50\text{ }^{\circ}\text{C}$, and an external (cold) box measuring $2.70\text{ m} \times 1.80\text{ m} \times 2.30\text{ m}$, simulating outdoor conditions with adjustable temperatures ranging from $-25\text{ }^{\circ}\text{C}$ to $+80\text{ }^{\circ}\text{C}$. The internal box is movable, allowing for the assembly of the tested building partitions between the two boxes. Figure 1 provides a general view of the climatic chamber at the Kielce University of Technology.



FIGURE 1. General view of the climatic chamber at the Kielce University of Technology

The system under investigation comprised four triple-pane windows adapted to be installed in a climatic chamber. Each window had a height of 87.5 cm and a length of 60.0 cm . The windows were mounted in a reinforced concrete wall using an aluminum frame (warm profile). The reinforced concrete wall was positioned between the cold and hot parts of the climatic chamber and was thermally insulated with a 20 cm layer of mineral wool on the cold side. A photograph of the experimental setup is presented in Figure 2.



FIGURE 2. Photograph of the climatic chamber testing plane

Figure 3 illustrates the cross-sectional diagrams of the tested triple-pane windows.

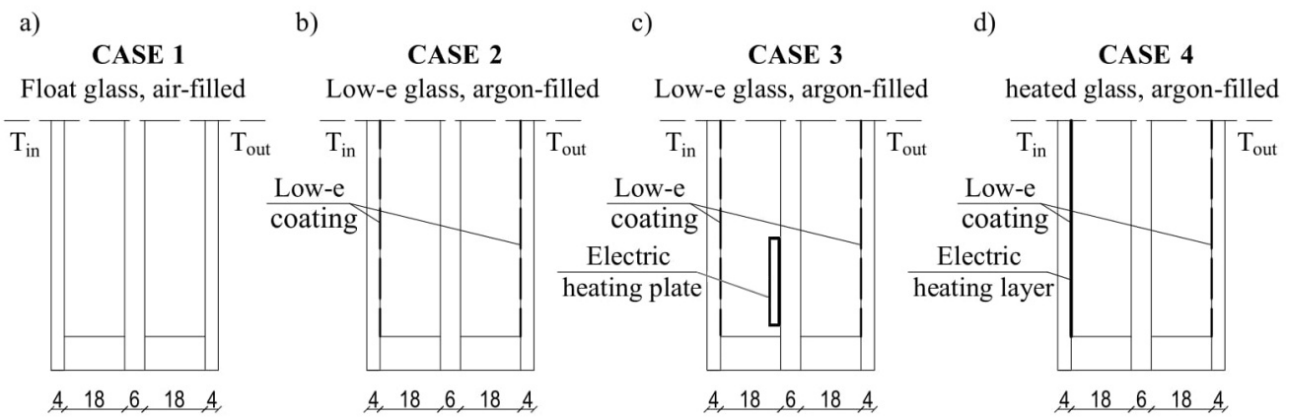


FIGURE 3. Cross-sectional diagrams of the tested triple-pane windows

As depicted in Figure 3, each outer and inner pane had a thickness (t) of 4 mm, while each central pane had a thickness of 6 mm. The width of the gaps between the panes was 18 mm. In Case 1 (Fig. 2a), the window consisted of three float glass panes with emissivity (ϵ) of 0.84 and thermal conductivity (k) of 0.92 W/mK, separated by air-filled gaps. Case 2 (Fig. 2b) examined the use of inert gas (argon) filling and low-emissivity coatings ($\epsilon = 0.17$) on the inner pane surface facing the gap. Case 3 (Fig. 2c) involved the installation of an electric heating plate in the lower part of the room-side gap, on the central pane, comprising resistance rods with a resistance of 50 Ω . The power supply wire, suitable for plugging into a 230 V socket, was routed from the inner side of the window frame. In Case 4 (Fig. 2d), the window operated by combining electric current with a low-emissivity metal oxide layer on the inner pane surface facing the gap. The power supply wire was connected to a thermostat that controlled the window's temperature.

Apparatus

The FHF04 foil heat flux sensor (Hukseflux) with sensitivity of $\Phi_i = 10.48 \mu V/(W/m^2)$ was attached to the lower, central and upper parts of the outer pane surface to monitor the heat flux density distribution of each window. The red dots in Figure 4 represent the sensor locations.

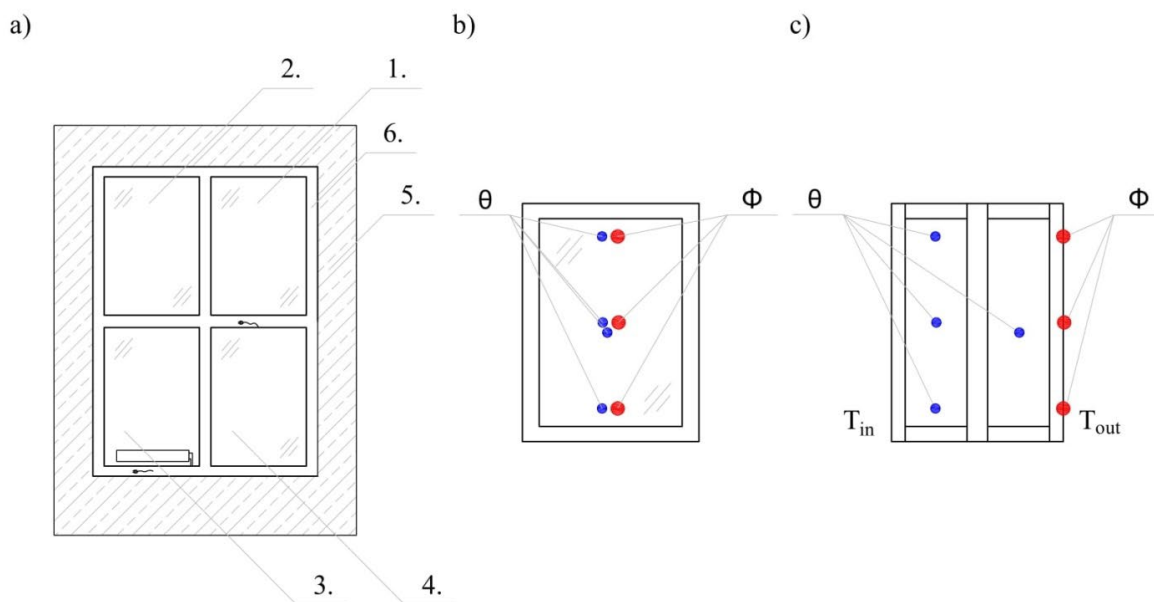


FIGURE 4. Cross-sectional diagrams of the tested triple-pane windows: 1, 2, 3, 4 – tested windows (case 1 to 4); 5 – reinforced concrete wall; 6 – aluminium frame; Φ – heat flux meters; θ – thermocouples; T_{in} – indoor box ambient, T_{out} – outdoor box ambient

The FHF04 sensors measured heat flux from conduction, radiation, and convection. Moreover, three K-type thermocouples were placed within the lower, central, and upper parts of the internal gap, and one K-type thermocouple was installed in the central part of the external gap in order to measure the cross-sectional temperature levels of each window. The blue dots in Figure 4 represent the thermocouple positions. The LI19 heat flux density data-logger (Hukseflux) was used to display and store the minimum, maximum and average heat flux measurements, along with corresponding date and time.

Additionally, the digital TM-947SD four-channels thermometer with data-logger (Lutron) was employed to record the temperature of the gas layer between the panes using K-type thermocouples. The Testo 872s thermal imager was utilized to capture thermal images for further analysis. Table 1 provides a summary of the apparatus employed in the experimental measurements.

Table 1. The apparatus used in the experimental measurements

| Instrument | Measurement | Sensitivity | Range |
|---|--|---|--|
| K-type thermocouples | temperature | 41 $\mu\text{V}/^\circ\text{C}$ | -100 $^\circ\text{C}$ to +400 $^\circ\text{C}$ |
| Foil heat flux sensors (FHF04, Hukseflux) | heat flux | 10.48 $\mu\text{V}/\text{W}/\text{m}^2$ | (-10 to +10) $\times 10^3 \text{ W}/\text{m}^2$ |
| Thermometer with data-logger (TM-947SD) | average temperature | - | - |
| Heat flux density data-logger (LI19, Hukseflux) | minimum, maximum and average heat flux | - | - |
| Thermal imager (Testo 872s) | thermography | 0.05 $^\circ\text{C}$ | -30 $^\circ\text{C}$ to +100 $^\circ\text{C}$; 0 $^\circ\text{C}$ to +650 $^\circ\text{C}$ |

Methods

The experimental study was conducted within the climatic chamber under constant conditions of an air temperature of 20 $^\circ\text{C}$ in the hot box and a humidity level of 50%. In order to demonstrate the effect of external temperature on heat flux through the windows, tests were carried out at three different cold box temperatures: -5 $^\circ\text{C}$, 0 $^\circ\text{C}$ and +5 $^\circ\text{C}$. The measurements were taken once both chambers reached a steady state, with the air temperature remaining constant and varying within 2% per hour. The tests continuously recorded results at 2-second intervals over a period of 1 hour. All measurements were conducted following the guidelines outlined in ISO 9869-1:2014.

The thermal transmittance (U) was calculated by dividing the average heat flux density on each part of the external glazing by the average temperature difference between the interior and exterior panes surfaces, as shown in equation (1) [15]. The thermal resistance (R) was calculated using equation (2) [15]

$$U = \frac{\sum_{j=1}^n q_j}{\sum_{j=1}^n (T_{sij} - T_{sej})}, \frac{\text{W}}{\text{m}^2\text{K}} \quad (1)$$

$$R = \frac{\sum_{j=1}^n (T_{sij} - T_{sej})}{\sum_{j=1}^n q_j}, \frac{\text{m}^2\text{K}}{\text{W}} \quad (2)$$

where:

U - thermal transmittance, $\text{W}/\text{m}^2\text{K}$;

R - thermal resistance, $\text{m}^2\text{K}/\text{W}$;

q - heat flux density, W/m^2 ;

T_{sij} – internal glazing surface temperature, °C;

T_{sej} – external glazing surface temperature, °C.

However, it is important to note that this test has certain limitations. Unfortunately, the climatic chamber used in this study is not equipped to investigate the impact of solar radiation. Consequently, the thermal performance of windows in the presence of solar radiation is not addressed in this study. Therefore, the results presented here should be considered comparable to reports with similar methodologies. Future research focusing on the influence of solar radiation on heat flux density distribution would be an interesting avenue to explore.

Results and discussion

The results of the experimental study are presented in both graphical and tabular formats. Figures 5-8 display the average heat flux density recorded on the lower, central and upper parts of external glazing of each window at an outside temperature of $T_{out} = -5^{\circ}\text{C}$. Additionally, Figure 9 shows a thermal image of Case 1, captured from the warm box side. The comparison between measurements and calculations is summarized in Table 2.

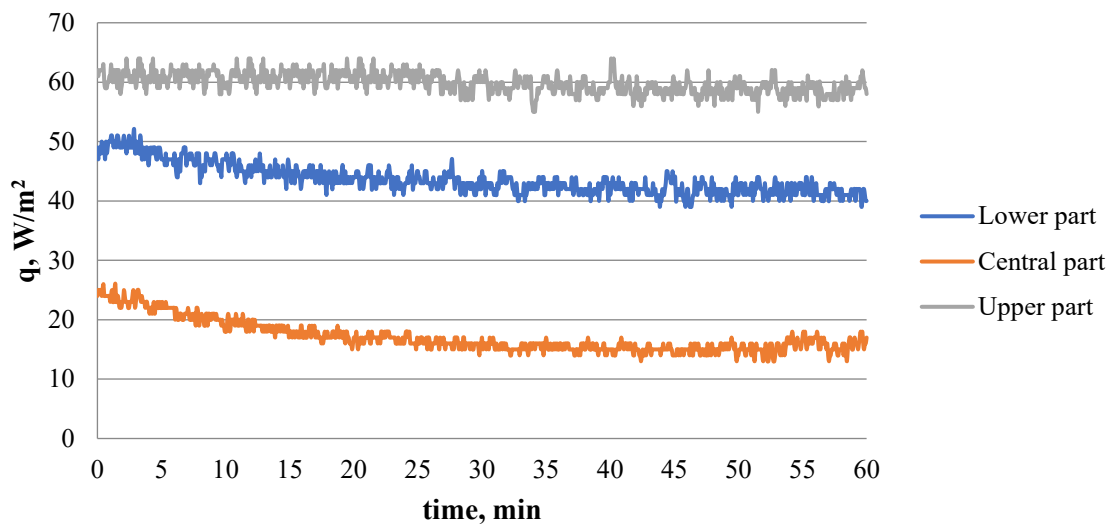


FIGURE 5. Average heat flux density values on the external glazing for the lower, central, and upper parts of the window in Case 1 ($T_{out} = -5^{\circ}\text{C}$)

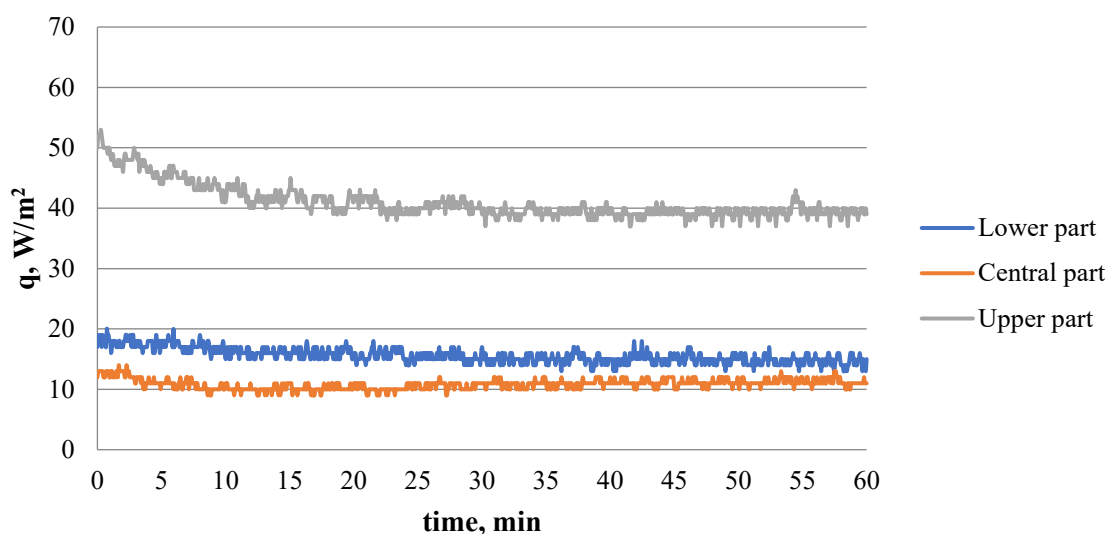


FIGURE 6. Average heat flux density values on the external glazing for the lower, central, and upper parts of the window in Case 2 ($T_{out} = -5^{\circ}\text{C}$)

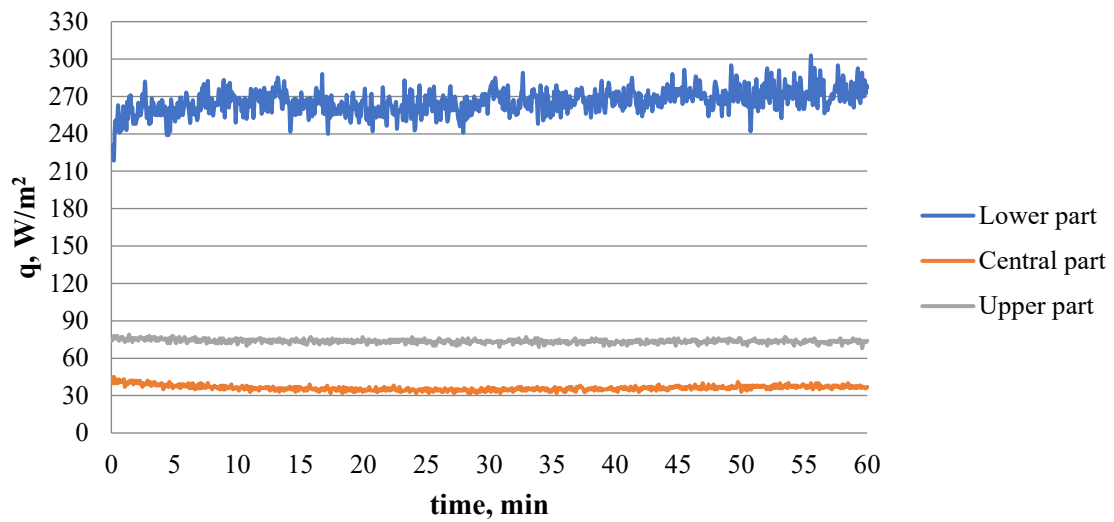


FIGURE 7. Average heat flux density values on the external glazing for the lower, central, and upper parts of the window in Case 3 ($T_{out} = -5\text{ }^{\circ}\text{C}$)

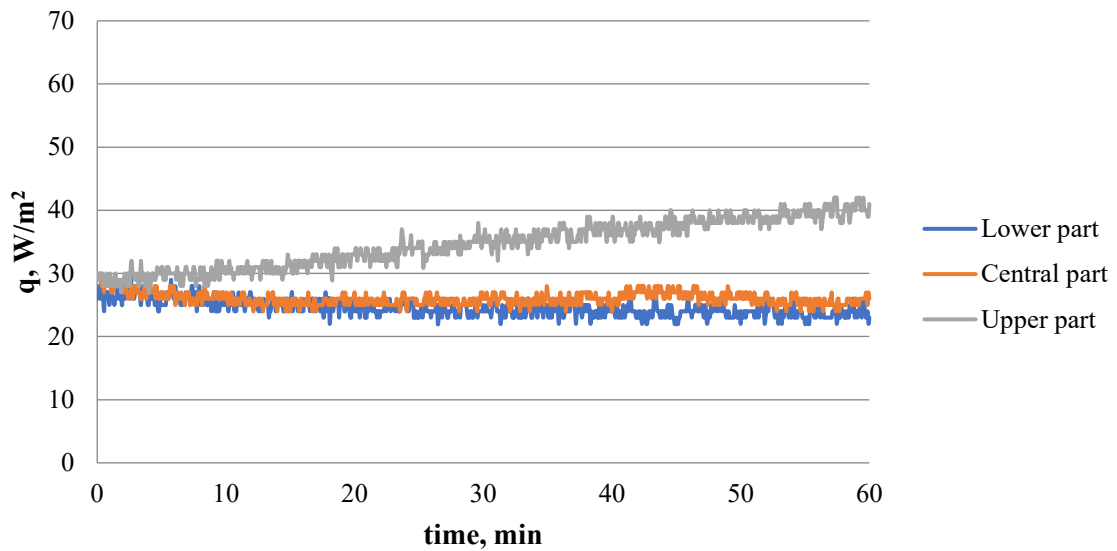


FIGURE 8. Average heat flux density values on the external glazing for the lower, central, and upper parts of the window in Case 4 ($T_{out} = -5\text{ }^{\circ}\text{C}$)

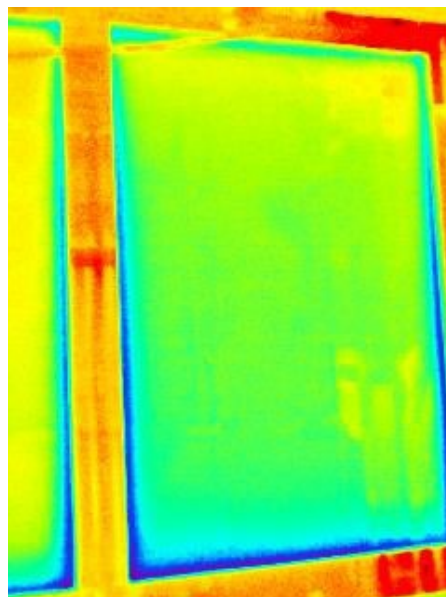


FIGURE 9. Thermal image of Case 1 captured from the warm box side

Table 2. Comparison of the measured average heat flux density and the calculated thermal transmittance and thermal resistance

| | Part | Case 1 | Case 2 | Case 3 | Case 4 |
|--------------------------------|---------|--------|--------|--------|--------|
| q , W/m ² | lower | 43.6 | 15.6 | 265.7 | 24.6 |
| | central | 18.0 | 10.8 | 36.1 | 26.0 |
| | upper | 59.8 | 41.0 | 73.7 | 34.6 |
| U -value, W/m ² K | lower | 2.422 | 0.918 | 9.194 | 1.166 |
| | central | 1.000 | 0.647 | 1.327 | 1.182 |
| | upper | 3.322 | 2.515 | 2.632 | 1.747 |
| R -value, m ² K/W | lower | 0.413 | 1.090 | 0.109 | 0.858 |
| | central | 1.000 | 1.546 | 0.753 | 0.846 |
| | upper | 0.301 | 0.398 | 0.380 | 0.572 |

Conclusions

This study investigated the heat flux density distribution in triple-pane windows filled with air and argon, considering the use of low-emissivity coatings and electric heating. Experimental analysis was conducted, and the results presented in Figures 5-8 indicated that heat flux densities remained relatively stable over time under constant outdoor temperature conditions without solar radiation. The variation in heat flux density across different parts of the glazing surface was primarily influenced by convection within the gas-filled gap between the panes and the differing thermal properties of the materials used (glass, spacer, and window frame). Based on the obtained results, the following conclusions can be drawn:

1. Steady-state conditions revealed significant discrepancies in heat flux density across different parts of the external glazing of each window, attributed to convective multicellular circulations within the gas layer.
2. The thermal transmittance varied among the lower, central, and upper parts of the external glazing of each window due to the distinct conductive properties of window materials and convection effects near the glazing and window edges.
3. For the air-filled triple-pane window with float glass panes (Case 1), the highest heat flux density value of 64 W/m² was observed on the upper part of the external glazing, while the lowest value of 14 W/m² was measured on the central part. This resulted in U -values that were more than 2 and 3 times higher in the lower and upper parts, respectively, compared to the central part.
4. The argon-filled window with low-emissivity coating (Case 2) exhibited a 35% reduction in heat flux density on the central part compared to the air-filled window (Case 1). The U -values were determined as 0.918, 0.647, and 2.515 W/m²·K for the lower, central, and upper parts, respectively (Case 2).
5. The use of local electric heating in the lower part of the central pane proved to be ineffective, resulting in an increase in heat flux density through the bottom of the window by over 17 times compared to Case 2. This led to the poorest thermal resistance among all tested windows.
6. Surface electric heating (Case 4) resulted in a more uniform distribution of heat flux densities along the height of the outer pane, with values of 24.6, 26.0 and 34.6 W/m² for the lower, central and upper parts, respectively. The thermal resistance values along the entire height of the window were the most consistent among the tested windows.
7. These findings emphasize the importance of considering the variability of thermal resistance across the entire height of windows. Therefore, considering this variability is crucial for an accurate calculation of the heat transfer coefficient.

References

- [1] Cuce E., Riffat S.B., *A state-of-the-art review on innovative glazing technologies*. Renewable and Sustainable Energy Reviews 2015, 41, 695-714, <https://doi.org/10.1016/j.rser.2014.08.084>.
- [2] Basok B.I., Davydenko B.V., Isaev S.A., Goncharuk S.M., Kuzhel L.N., *Numerical modeling of heat transfer through a triple-pane window*, Journal of Engineering Physics and Thermophysics 2016, 89(5), 1277-1283, <https://doi.org/10.1007/s10891-016-1492-7>.
- [3] Basok B., Davydenko B., Novikov V.G., Pavlenko A.M., Novitska M.P., Sadko K., Goncharuk S.M., *Evaluation of heat transfer rates through transparent dividing structures*. Energies 2022, 15, 4910, <https://doi.org/10.3390/en15134910>.
- [4] Nia M.F., Nassab S.A.G., Ansari A.B., *Transient numerical simulation of multiple pane windows filling with radiating gas*, International Communications in Heat and Mass Transfer 2019, 108, 104291, <https://doi.org/10.1016/j.icheatmasstransfer.2019.104291>.
- [5] Basok B., Davydenko B., Zhelykh V., Goncharuk S., Kuzhel L., *Influence of low-emissivity coating on heat transfer through the double-glazing windows*, Building physics in theory and practice (Fizyka budowli w teorii i praktyce) 2016, 8(4), 5-8.
- [6] Arıcı M., Kan M., *An investigation of flow and conjugate heat transfer in multiple pane windows with respect to gap width, emissivity and gas filling*. Renewable Energy 2015, 75, 249-256, <https://doi.org/10.1016/j.renene.2014.10.004>.
- [7] Rojewska-Warchał M., *The influence of glazing type, frame profiles, shape and size of the window of the final value of window thermal transmittance U*. Czasopismo Techniczne, Architektura 2014, 8A(15), 199-206, <https://doi.org/10.4467/2353737XCT.14.206.3294>.
- [8] Arıcı M., Karabay H., Kan M., *Flow and heat transfer in double, triple and quadruple pane windows*. Energy and Buildings 2015, 86, 394-402, <https://doi.org/10.1016/j.enbuild.2014.10.043>.
- [9] Aguilar-Santana J.L., Velasco-Carrasco M., Riffat S., *Thermal Transmittance (U-value) Evaluation of Innovative Window Technologies*. Future Cities and Environment 2020, 6(1). <http://doi.org/10.5334/fce.99>.
- [10] Cuce E., *Accurate and reliable U-value assessment of argon-filled double glazed windows: A numerical and experimental investigation*. Energy and Buildings 2018, 171, 100-106, <https://doi.org/10.1016/j.enbuild.2018.04.036>.
- [11] Pavlenko A.M., Sadko K., *Evaluation of Numerical Methods for Predicting the Energy Performance of Windows*. Energies 2023, 16, 1425, <https://doi.org/10.3390/en16031425>.
- [12] Lee R., Kang E., Lee H., Yoon J., *Heat Flux and Thermal Characteristics of Electrically Heated Windows: A Case Study*. Sustainability 2022, 14, 481, <https://doi.org/10.3390/su14010481>.
- [13] Gloriant F., Joulin A., Tittlein P., Lassue S., *Using heat flux sensors for a contribution to experimental analysis of heat transfers on a triple-glazed supply-air window*. Energy 2021, 215(A), 119154, <https://doi.org/10.1016/j.energy.2020.119154>.
- [14] Gori V., Marincioni V., Biddulph P., Elwell C.A., *Inferring the thermal resistance and effective thermal mass distribution of a wall from in situ measurements to characterise heat transfer at both the interior and exterior surfaces*. Energy and Buildings 2017, 135, 398-409, <https://doi.org/10.1016/j.enbuild.2016.10.043>.
- [15] BSI. 2014. ISO 9869-1:2014 – Thermal insulation — Building elements — Insitu measurement of thermal resistance and thermal transmittance; Part 1: Heat flow meter method.